

INVESTIGATION OF FINE SCALE STRUCTURES IN A TURBULENT JET BY USING CINEMATOGRAPHIC PARTICLE IMAGE VELOCIMETRY

Bharathram Ganapathisubramani
Department of Aeronautics,
Imperial College London,
Prince Consort Road, London, SW7 2AZ
g.bharath@imperial.ac.uk

Noel T Clemens
Department of Aerospace Engineering and Engineering Mechanics,
The University of Texas at Austin
210 East 24th Street, Austin, TX 78712
clemens@mail.utexas.edu

ABSTRACT

Cinematographic stereoscopic PIV measurements were performed to resolve small- and intermediate-scales in the far field of an axisymmetric co-owing jet. Measurements were performed in a plane normal to the axis of the jet and the time-resolved measurement was converted to quasi-instantaneous three-dimensional data by using Taylor's hypothesis. The quasi-instantaneous three-dimensional data enabled computation of all nine components of the velocity gradient tensor over a volume. Iso-surfaces of swirling strength (a vortex identification parameter) in the volume reveal that, in agreement with direct numerical simulation results, the intense vortex structures are in the form of elongated 'worms' with characteristic diameter of approximately 10η and characteristic length of $60-100\eta$. Iso-surfaces of intense dissipation show that the most dissipative structures are in the form of sheets and are associated with clusters of vortex tubes. The largest length scale of dissipation sheets is of order 60η and the characteristic thickness (in a plane normal to the axis of the sheet) is about 10η .

INTRODUCTION

The structure of intermediate- and fine-scales in turbulent shear flows is a long-standing research problem and remains one of the most challenging aspects of turbulent flows. The dynamics of intermediate- and fine-scales of turbulent shear flows are important to turbulence theory and to the development and validation of sub-grid scale models used in large-eddy simulations of shear flows.

Several experimental and computational studies have investigated the fine scales in a turbulent flow by computing various statistical estimates like scaling exponents of probability density distributions, structure functions, skewness and flatness for various quantities like vorticity, circulation and dissipation and have statistically characterized the small-scale motions (see Sreenivasan & Antonia 1997).

A complete analysis of the three-dimensional structure of dissipation, vorticity and other gradient quantities in turbulent flows requires detailed simultaneous three dimensional velocities and velocity gradient information. Such information has been derived mainly from Direct Numerical Simulations (DNS) of turbulence. Although, previous experimental and analytical studies provide a range of geometric models for the fine-scale structures, DNS studies of isotropic

turbulence appear to agree that intense regions of vorticity tend to form tubes, also called 'worms' (for example, Siggia 1981; Kerr 1985; Ashurst *et al.* 1987; Vincent & Meneguzzi 1991; Ruetsch & Maxey 1991; Jimenez *et al.* 1993). Some researchers investigated the relationship between vorticity and dissipation (Kerr 1985; Brachet 1991; Kida & Ohkitani 1992; Vincent & Meneguzzi 1994) by visualizing these quantities, obtained from DNS datasets, simultaneously. These studies concluded that intense dissipative structures are found in the vicinity of intense vortex cores (or 'worms'). However, the exact structure of intense dissipation is not clearly defined. Brachet (1991) indicated that the regions of intense enstrophy are spatially more concentrated than the energy dissipation. Other studies found that the shape of the kinetic energy dissipation field is more complicated since it contains sheet-, line- and blob-like structures (Siggia 1981; Kerr 1985; Yamamoto & Hosokawa 1988).

Most experimental studies in the literature rely on point measurements or flow visualization techniques to speculate on the three-dimensional structure of the flow field. Therefore those studies cannot provide insight into the instantaneous spatial structure of the finest scales. Tsurikov (2003) performed two component particle image velocimetry measurements to resolve small- and intermediate-scales of the flow and concluded that intense regions of kinetic energy dissipation possessed sheet-like structures. However, planar measurements cannot capture the complete spatial structure of the flow field. Recently, Mullin & Dahm (2006a) performed dual-plane stereoscopic experiments to study the fine- and intermediate scales of a turbulent shear flow. The technique enables computation of all nine velocity gradients over a plane; however, the information is available only over a plane and therefore cannot completely describe the three-dimensional structure. Zeff *et al.* (2003) reconstructed a three-dimensional velocity field based on simultaneous high-speed PIV measurements in three different planes of a small cube. The authors found that dissipation and enstrophy are spatially and temporally separated and are largely intermittent. Su & Dahm (1996) performed scalar imaging velocimetry where the complete velocity gradient tensor of the flow field was obtained by inversion of the conserved scalar transport equation. The authors investigated three-dimensional flow fields of enstrophy and dissipation and concluded that both quantities are relatively 'spotty' with large values occurring very rarely. The field of view of the

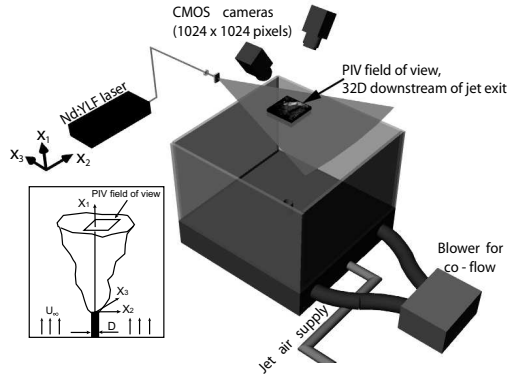


Figure 1: Experimental setup.

above mentioned study was approximately $15\eta \times 15\eta$ and as a result they were unable to resolve the intermediate scales of the flow field.

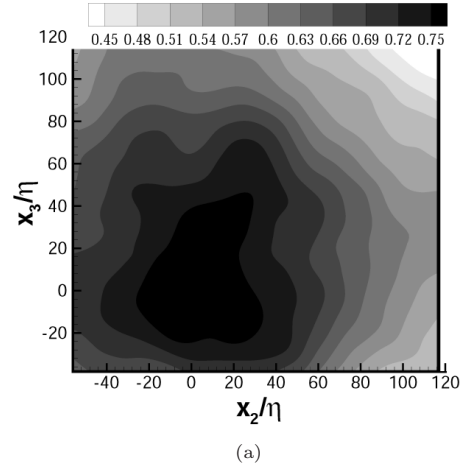
In the present study, time-resolved stereoscopic particle image velocimetry is utilized to measure three components of velocity in a plane and Taylor's hypothesis is employed to reconstruct a quasi-instantaneous volume of data. Experiments were performed in the far field of an axisymmetric co-flowing jet where the Kolmogorov scale is large enough so that the dissipation scales can be resolved. The pseudo-three-dimensional data are used to compute the complete velocity gradient tensor along with the three components of vorticity and other derived quantities such as three-dimensional dissipation rates. The goal of this study is to experimentally investigate the three-dimensional intermediate- and fine-scale spatial structure of vorticity and dissipation.

EXPERIMENTAL SETUP

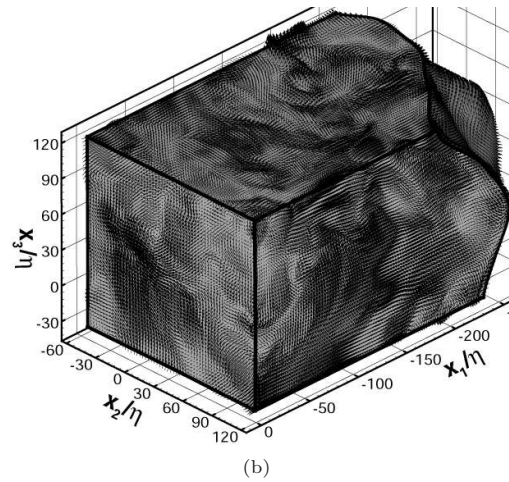
Cinematographic stereoscopic PIV experiments were performed in an "end-view" plane in the far-field of a mildly co-flowing axisymmetric turbulent air jet. A schematic of the experimental setup is shown in figure 1. The following are some relevant length scales at the measurement location: Jet half width ($\delta_{1/2}$) = 126 mm, Taylor micro-scale (λ) = 13.8 mm and Kolmogorov scale (η) = 0.45 mm. The Reynolds number based on jet exit velocity and diameter $Re_D = 5100$ and the Reynolds number based on Taylor micro-scale $Re_\lambda \approx 150$.

The cinematographic PIV system (shown in figure 1) consists of a Nd:YLF laser (Coherent Evolution-90) with an output wavelength of 527 nm and a pair of high-framing rate 1024×1024 pixel resolution CMOS cameras (Photron FASTCAM-Ultima APX) that were operated at a rate of 2 kHz. Glycerin droplets were seeded into the co-flow and subsequently entrained by the developing jet. The seed particles were illuminated by a laser sheet and the scattered light was captured by the two CMOS cameras in stereoscopic arrangement.

Velocity vectors were computed from the cinematographic images from each camera and were then combined with suitable magnification factors to compute all the three velocity components. The resolution of the resulting stereoscopic vector field is about $3\eta \times 3\eta$. Taylor's hypothesis with a convection velocity equal to the local mean axial velocity $\bar{u}_1(x_2, x_3)$ (u_1 , u_2 and u_3 are velocity components along x_1 , x_2 and x_3 directions respectively) was utilized to reconstruct a quasi-instantaneous space-time volume of data. The con-



(a)



(b)

Figure 2: (a) Mean streamwise velocity in $x_2 - x_3$ plane. (b) Sample vector field from a quasi-instantaneous space-time volume computed using Taylor's hypothesis.

vection velocity (i.e., the mean axial velocity) varies over the $x_2 - x_3$ plane as shown in figure 2(a) and consequently the axial coordinates are different for different regions of the jet. Note that the mean velocity contours are not round indicating that the data have not statistically converged.

The total size of the reconstructed quasi-instantaneous volume $x_1 \times x_2 \times x_3 = 1300\eta \times 160\eta \times 160\eta$ ($5\delta_{1/2} \times 0.6\delta_{1/2} \times 0.6\delta_{1/2}$). Figure 2(b) shows three-dimensional velocity vectors from a sample part of the total volume. The field of view of the volume in figure 2(b) is $250\eta \times 160\eta \times 160\eta$ ($0.8\delta_{1/2} \times 0.6\delta_{1/2} \times 0.6\delta_{1/2}$). The figure clearly shows a distorted grid conforming to the variations in the local convection velocity. The axial coordinates near the jet center are stretched while the coordinates away from the jet centerline (at larger radial locations) are compressed since the mean jet axial velocity (\bar{u}_1) is higher near the center and is lower at the periphery.

The pseudo-volume was used to compute all nine components of the velocity gradient tensor. A second order central difference technique was employed to compute all gradients. Additional details of the experimental technique and validation for the use of this technique to compute all nine components of the velocity gradient tensor can be found in Ganapathisubramani *et al.* (2007a).

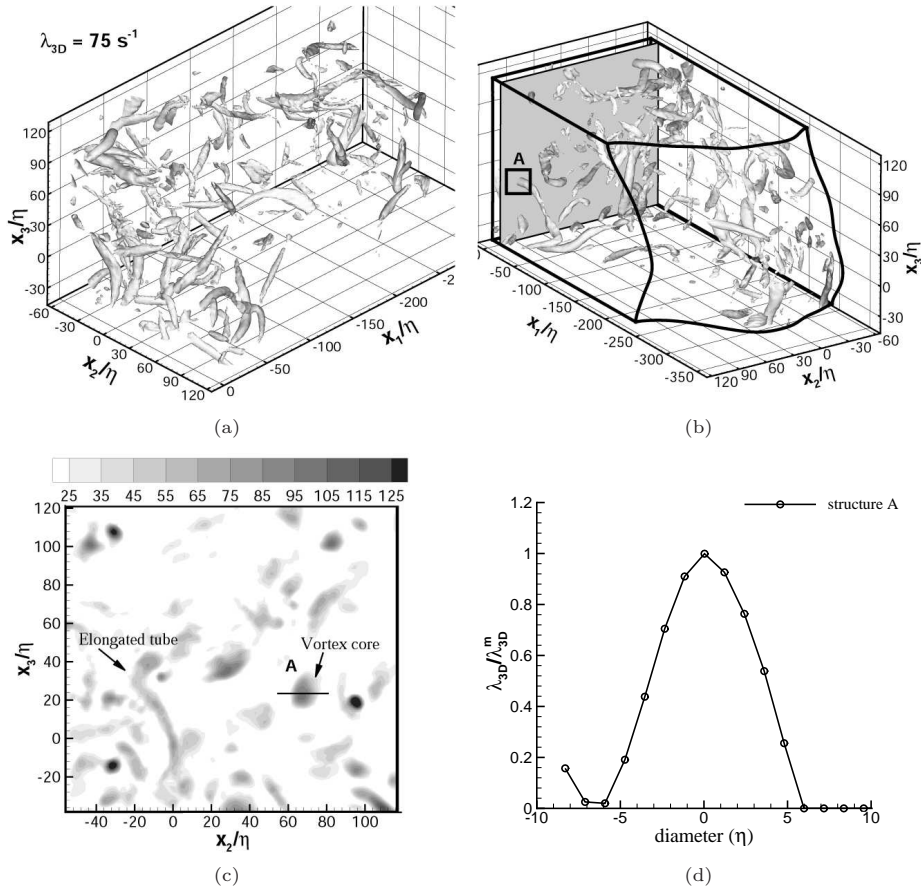


Figure 3: Instantaneous vortex structure. (a)-(d) Different views of iso-surfaces of $\lambda_{3D}=75\text{s}^{-1}$. (e) Contours of λ_{3D} on a plane normal to the vortex tube marked (A). The plane is shown in figure 3(d). (f) Swirling strength profiles across selected vortex cores. The profiles are along a diametric line in a plane normal to the axis of the core.

RESULTS

The structure of the vorticity and dissipation fields can be studied by rendering instantaneous iso-surfaces of ω and ϵ over a volume. This analysis is similar to those performed in previous DNS based studies (Siggia 1981; Yamamoto & Hosokawa 1988; Vincent & Meneguzzi 1991; Jimenez *et al.* 1993).

The structure of the vorticity field can be studied by examining the contours/iso-surfaces of a vortex identification parameter that is based on the local flow topology. Various studies in the literature have compared and contrasted several vortex identification parameters (for example, Jeong & Hussain 1995; Cucitore, Quadrio & Baron 1999), but there is no general consensus on an optimal parameter to isolate vortex cores. Zhou *et al.* (1999) used swirling strength (λ_{ci}^2), which is the square of the imaginary part of the eigenvalue of the three-dimensional velocity gradient tensor, to visualize vortex cores in a DNS dataset of channel flow. They found that this quantity, which isolates regions of fluid swirling about an axis, can be used to visualize vortical structures. In this study, the swirling strength, defined as $\lambda_{3D} = |\lambda_{ci}|$, is used to visualize swirling regions in the flow. Although swirling strength is used to visualize the structure of swirling/rotational motion, it must be noted that the use of other vortex identification parameters like enstrophy (or alternatively, the second invariant of the velocity gradient tensor or λ_2 as defined in Jeong & Hussain 1995) does not alter the results or conclusions presented in this section.

Figures 3(a)-3(b) show iso-surfaces of $\lambda_{3D} = 75\text{s}^{-1}$ (where mean and *rms* values of λ_{3D} correspond to 15 s^{-1} and 20 s^{-1} respectively). Both figures show that the vortex structures are organized in tube-like structures, which is consistent with observations made in previous DNS studies (Siggia 1981; Ashurst *et al.* 1987; Ruetsch & Maxey 1992; Jimenez *et al.* 1993). These tube-like structures were named ‘worms’ by Jimenez *et al.* (1993) where the authors indicated that these ‘worms’ were the most intense realizations of background vorticity (i.e., the magnitude of vorticity in these tubes is much larger than root-mean-square of vorticity).

Further investigation of the size of the ‘worms’ was conducted by extracting a cross-sectional plane of data normal to the axis of one elongated worm (marked A in figure 3b). Figure 3(c) shows contours of λ_{3D} in the cross sectional plane normal to the axis of a ‘worm’. The contours indicate a circular profile for the vortex core. Figure 3(c) also shows other vortex structures that cut across the plane. In particular, the cross section of an elongated tube (marked in the figure) indicates the typical length of these worms to be approximately $60 - 100\eta$. Figure 3(d) shows a diametric profile of $\lambda_{3D}/\lambda_{3D}^m$ along the line marked in figure 3(c) (where λ_{3D}^m is the maximum value of λ_{3D} within the vortex core). The diameter of the core marked A in figure 3(d) was found to be 9η . Examination of other diametric profiles indicate that the core diameters of these structures vary between 6η and 14η and is consistent with the results of Jimenez *et al.*

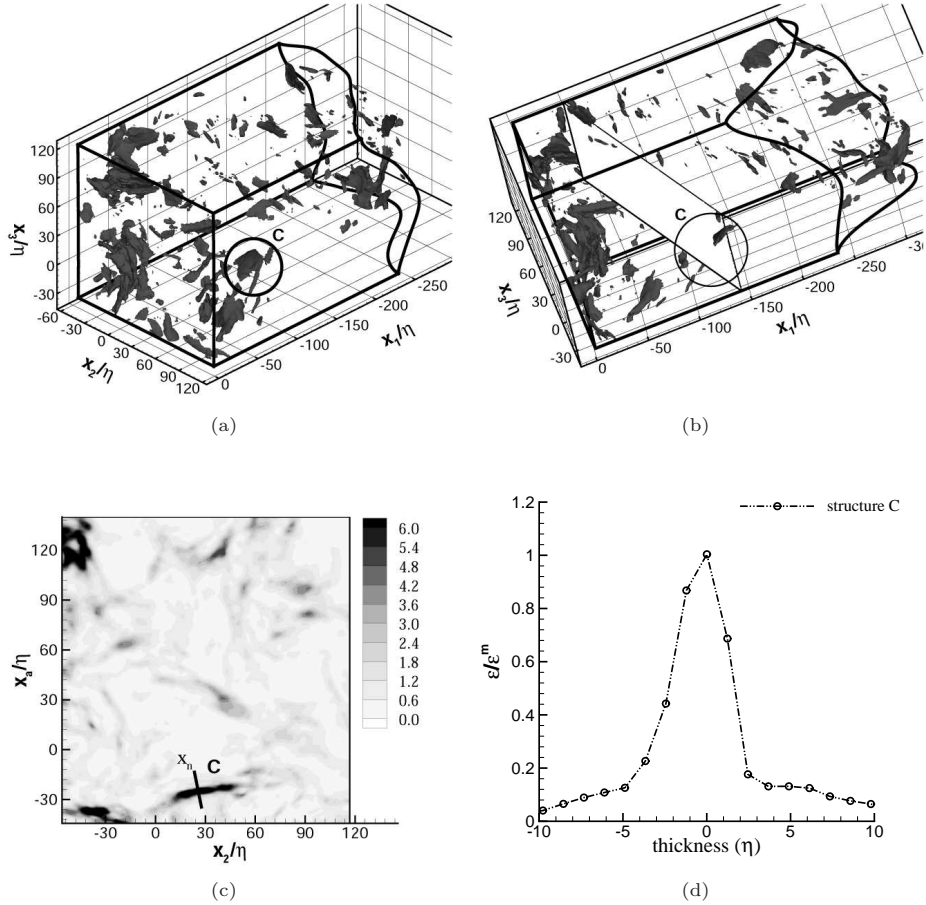


Figure 4: Instantaneous vortex structure. (a)-(b) Different views of iso-surfaces of $\epsilon=0.4\text{m}^2\text{s}^{-3}$. (c) Contours of $\epsilon/\bar{\epsilon}$ on a plane normal to the dissipation sheet marked (C). The plane is shown in figure 4(b) and (d) Thickness profile of dissipation sheet along a line normal to the structure in a plane that is normal to the sheet as marked in figure 4(c).

(1993) who found that the diameter of intense vortex worms was nominally 8η . The observation that the worm core diameter is significantly larger than the Kolmogorov scale is also consistent with the “strain-limited diffusion scale for vorticity”, λ_ν , defined by Buch & Dahm (1996). Buch & Dahm (1998) and Mullin & Dahm (2006b) inferred from scalar dissipation measurements and dual-plane stereoscopic measurements respectively, that the smallest scale of vortical structures is λ_ν , which is about six times larger than the Kolmogorov scale.

The reconstructed quasi-instantaneous volume also provides an opportunity to investigate the three-dimensionality of dissipative structures. The instantaneous three-dimensional structure of dissipation was investigated by examining iso-surfaces of ϵ . Figure 4(a) shows iso-surfaces of $\epsilon = 0.4 \text{ m}^2/\text{s}^3$, which is about six times the value of mean dissipation. Therefore, these iso-surfaces represent intense dissipative regions in the flow field. Figure 4(a) seems to show a wide range of shapes and forms for the dissipation structure that vary from sheets to blobs. This observation is consistent with the previous studies by Siggia (1981) and Yamamoto & Hosokawa (1988) where three-dimensional visualization of kinetic energy dissipation obtained from DNS data was found to be complex, containing sheet-, line- and blob-like structures.

The structure of dissipation can be examined in detail by isolating individual structures. Consider a characteristic blob marked C in figure 4(a). From this perspective this

structure appears to be a blob of intense dissipation. However, when viewed from a different perspective as shown in figure 4(b), this blob marked C is in fact a sheet-like structure with finite thickness. Figures 4(a) and 4(b) also reveal other structures (not marked) that are sheet-like, but appear to be blobs when viewed from other perspectives. Movie sequences generated by rotating the pseudo-volume along different axes reveal that most blobs (seen in figure 4a) are in fact sheets.

To further investigate the thickness of the sheets of dissipation, a plane normal to the axis of the dissipation sheet marked C is extracted as shown in figure 4(b). This extracted plane ($x_a - x_2$, x_a is the coordinate along the plane shown in figure 4b) is at an angle $\xi = 60^\circ$, where ξ is the angle made by the plane with $x_1 - x_2$ plane. Figure 4(c) shows contours of ϵ in the extracted $x_a - x_2$ plane (the coordinate $x_a = x_3 \sec \xi$). The contours reveal that the dissipation sheet has a finite thickness. The contours also indicate that the largest length scale of these sheets are of order 60-100 η . For example, the length of the sheet marked C is approximately 60 η in the x_2 direction. The thickness of the dissipation sheet can be deduced by plotting the profile of ϵ along the line marked x_n , in figure 4(d). Buch & Dahm (1998) investigated the thickness of scalar dissipation structures and the thickness was determined by the width where the dissipation falls to 20% of the local maximum value. Following the above mentioned definition for thickness, the profile, ϵ/ϵ^m versus x_n (where ϵ^m is the maximum value of dissipation in

the sheet) in figure 4(d) shows that the thickness of sheet **C** is approximately 10η . Other thickness profiles extracted from planes normal to the structures indicate that the thickness of dissipation sheets varies between 6η and 12η .

The iso-surfaces of ϵ and λ_{3D} can be visualized simultaneously to investigate the instantaneous relationship between the vortical and dissipation structures. Figure 5(a) show iso-surfaces of $\epsilon = 0.4\text{m}^2/\text{s}^3$ (in black) and $\lambda_{3D} = 75\text{s}^{-1}$ (in white). The figure show that intense dissipative regions are not coincident with regions of intense λ_{3D} , rather, the elongated tubes of intense vorticity are surrounded by the sheets of intense dissipation (Kerr 1985; Vincent & Meneguzzi 1994; Pradeep & Hussain 2006). This fact can be further quantified by computing joint probability density functions of λ_{3D} and ϵ (see Ganapathisubramani *et al.* 2007*b* for details).

Three different regions where dissipation is found in the vicinity of vortex tubes are marked in figures 5(a). Regions marked **A** and **B** possess a nested structure of multiple vortex tubes with crumpled dissipation sheets located between the tubes, whereas, the region marked **C** does not have multiple tubes. Upon increasing the threshold for dissipation iso-surfaces to $10\bar{\epsilon}$, the dissipation sheet marked **C** just disappears, suggesting that extremely intense dissipative regions occur mostly between multiple vortex tubes where the strain fields induced by these vortex tubes overlap (please see Ganapathisubramani *et al.* 2007*b* for details).

The local structure of dissipation around a vortex tube can be further investigated by considering a zoomed in view of the nested structure marked **A** in figure 5(b). Figure 5(b) reveals a closer look at the iso-surfaces of λ_{3D} and ϵ in region **A**, and indicates that the sheet of dissipation is crumpled and nested between two or more cores. Contours of ϵ in a cross sectional plane normal to a vortex core is shown in figure 5(c). The contours show that the dissipation structure around the vortex core is in the form of an annulus, however, the annular region is not radially symmetric. Figure 5(d) shows contours of intermediate strain rate (β) in the same cross-sectional plane. The figure indicates that the intermediate strain possesses intense positive values in the regions of intense dissipation. This observation is consistent with the results based on joint p.d.fs between ϵ and β , where higher values of dissipation was found to be concurrent with higher values of positive β (see Ganapathisubramani *et al.* 2007*b*). This provides further support for the presence of sheet-like dissipative structures since the sheet structure is induced by the presence of two extensive strains (i.e. $\alpha > 0$ and $\beta > 0$, where α is the largest principal strain and is always positive).

CONCLUSIONS

Cinematographic stereoscopic PIV experiments were performed to resolve small- and intermediate-scales (scale: $\approx 3\eta - 160\eta$) in the far field of an axisymmetric co-flowing jet. Measurements were performed in a plane normal to the axis of the jet. The time-resolved velocity measurements were then converted to a quasi-instantaneous three-dimensional reconstruction of the jet. Taylor's hypothesis was applied to the data along the jet axial direction to reconstruct the axial spatial extent. The availability of quasi-three-dimensional data enabled computation of all nine components of the velocity gradient tensor over the volume, which could be utilized to investigate the structure of dissipation and vorticity.

The availability of quasi-instantaneous space-time vol-

umes of data enable visualization of iso-surfaces of strain rate, vorticity and dissipation that can shed insight in to the structure of intermediate- and fine-scale of turbulent flow. Investigation of iso-surfaces of swirling strength in a quasi-instantaneous volume reveals that the intense vortex structures are elongated in one direction and appear to be in the form of 'worms'. A cross-sectional view of these 'worms' indicates that these vortex cores have a diameter of approximately 10η , consistent with results from DNS of isotropic turbulence (for example, Siggia 1981; Jimenez *et al.* 1993). The characteristic length of the worms is about $60-100\eta$.

Iso-surfaces of dissipation show that the regions of intense dissipative regions are in the form of sheets and are coincident with positive values of intermediate strain. The dissipation sheets are found to be in the neighborhood of intense vortex tubes and extremely intense dissipation sheets ($\epsilon > 10\bar{\epsilon}$) appear in the vicinity of multiple nested vortex tubes. Intense dissipation does not occur within a vortex tube but results from the interaction between the nested groups of vortex tubes. Analysis of thickness profiles of the dissipation sheets (in a plane normal to the axis of the sheet) indicates that the thickness varies between 6η and 12η . The largest length scale of these sheets (length or width) extend to 60η .

Visualization of quasi-instantaneous data indicates that the intense dissipative structures and vortex tubes possess physical scales that are much larger than the Kolmogorov scale, which is consistent with the findings based on investigation of energy and dissipation spectra.

REFERENCES

- ASHURST, W. T., KERSTEIN, A. R., KERR, R. M. & GIBSON, C. H. 1987 Alignment of vorticity and scalar gradient with strain rate in simulated Navier-Stokes turbulence. *Phys. Fluids* **30**, 2343–2353.
- BRACHET, M. E. 1991 Direct simulation of three-dimensional turbulence in the Taylor-Green vortex. *Fluid Dyn. Res.* **8(1-4)**, 1–8.
- BUCH, K. A. & DAHM, W. J. A. 1996 Experimental study of the fine-scale structure of conserved scalar mixing in turbulent shear flows. Part 1. $Sc \ll 1$. *J. Fluid Mech.* **317**, 21–71.
- BUCH, K. A. & DAHM, W. J. A. 1998 Experimental study of the fine-scale structure of conserved scalar mixing in turbulent shear flows. Part 2. $Sc \approx 1$. *J. Fluid Mech.* **364**, 1–29.
- CUCITORE, R., QUADRIO, M. & BARON, A. 1999 On the effectiveness and limitations of local criteria for the identification of a vortex. *Eur. J. Mech. B/Fluids* **18**, 261–282.
- GANAPATHISUBRAMANI, B., LAKSHMINARASIMHAN, K. & CLEMENS, N. T. 2007*a* Determination of complete velocity gradient tensor using cinematographic stereoscopic particle image velocimetry in the far field of a turbulent jet. *Exp. Fluids* **In press**.
- GANAPATHISUBRAMANI, B., LAKSHMINARASIMHAN, K. & CLEMENS, N. T. 2007*b* Investigation of three-dimensional structure of fine-scales in a turbulent jet by using cinematographic stereoscopic PIV. *J. Fluid Mech.* **Under review**.
- JEONG, J. & HUSSAIN, F. 1995 On the identification of a vortex. *J. Fluid Mech.* **258**, 69–94.
- JIMENEZ, J., WRAY, A. A., SAFFMAN, P. G. & ROGALLO, R. S. 1993 The structure of intense vorticity in isotropic turbulence. *J. Fluid Mech.* **255**, 65–90.
- KERR, R. M. 1985 Higher-order derivative correlations and the alignment of small-scale structures in isotropic numerical turbulence. *J. Fluid Mech.* **153**, 31–58.

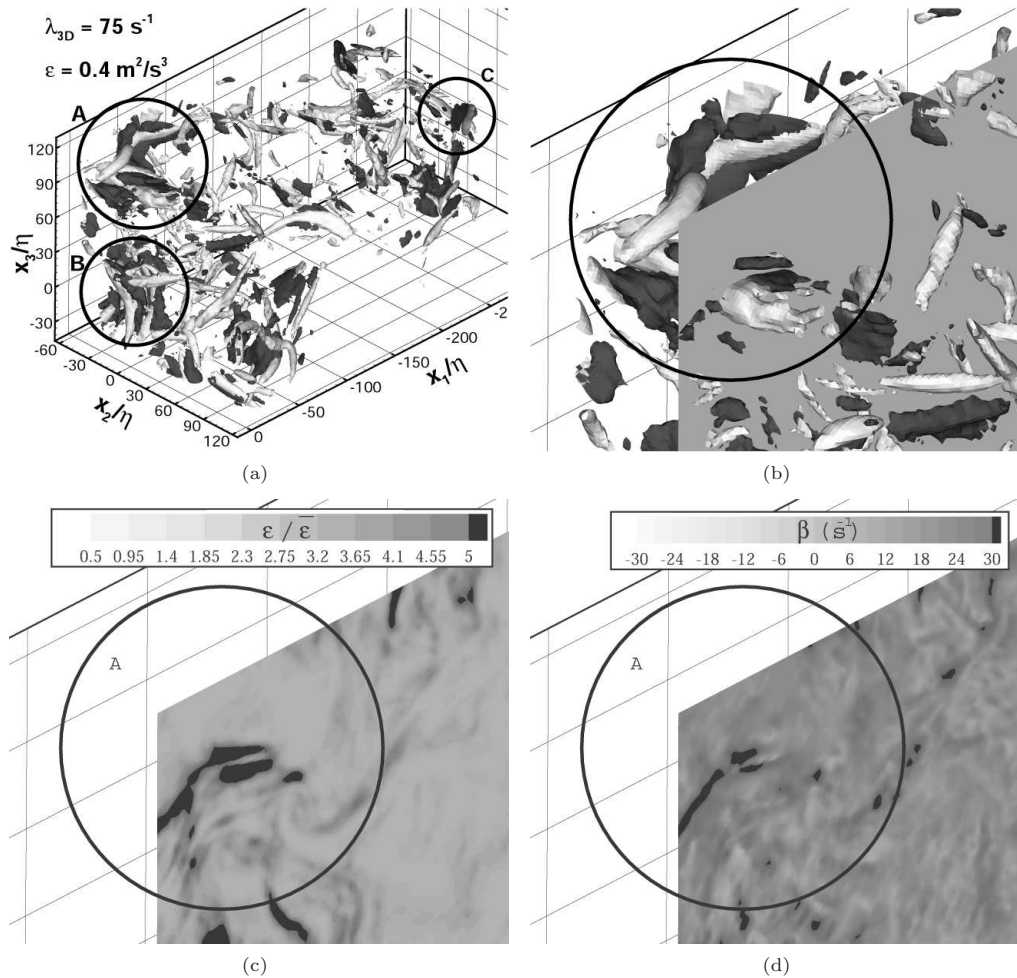


Figure 5: Instantaneous vortex structure. (a)-(d) Different views of iso-surfaces of $\lambda_{3D}=75\text{s}^{-1}$. (e) Contours of λ_{3D} on a plane normal to the vortex tube marked (A). The plane is shown in figure 3(d). (f) Swirling strength profiles across selected vortex cores. The profiles are along a diametric line in a plane normal to the axis of the core.

KIDA, S. & OHKITANI, K. 1992 Spatiotemporal intermittency and instability of a forced turbulence. *Phys. Fluids* **4**(5), 1018–1027.

MULLIN, J. A. & DAHM, W. J. A. 2006a Dual-plane stereo particle image velocimetry measurements of velocity gradient tensor fields in turbulent shear flow. I, Accuracy assessments. *Phys. Fluids* **18-035101**, 1–18.

MULLIN, J. A. & DAHM, W. J. A. 2006b Dual-plane stereo particle image velocimetry measurements of velocity gradient tensor fields in turbulent shear flow. II, Experimental results. *Phys. Fluids* **18-035102**, 1–28.

PRADEEP, D. S. & HUSSAIN, F. 2006 Transient growth of perturbations in a vortex column. *J. Fluid Mech.* **550**, 251–288.

RUETSCH, G. R. & MAXEY, M. R. 1991 Small-scale features of vorticity and passive scalar fields in homogeneous isotropic turbulence. *Phys. Fluids* **3**(6), 1587–1597.

RUETSCH, G. R. & MAXEY, M. R. 1992 The evolution of small-scale structures in homogeneous isotropic turbulence. *Phys. Fluids* **4**(12), 2747–2760.

SIGGIA, E. D. 1981 Numerical study of small-scale intermittency in three-dimensional turbulence. *J. Fluid Mech.* **107**, 375–406.

SREENIVASAN, K. R. & ANTONIA, R. A. 1997 The phenomenology of small-scale turbulence. *Annu. Rev. Fluid Mech.* **29**, 435–472.

SU, L. K. & DAHM, W. J. A. 1996 Scalar imaging velocimetry measurements of the velocity gradient tensor field in turbulent flows. II. Experimental results. *Phys. Fluids* **8**, 507–521.

TSURIKOV, M. 2003 Experimental investigation of the fine-scale structure in turbulent gas-phase jet flows. PhD thesis, Department of Aerospace Engineering and Engineering Mechanics, The University of Texas at Austin, USA.

VINCENT, A. & MENEGUZZI, M. 1991 The spatial structure and statistical properties of homogeneous turbulence. *J. Fluid Mech.* **225**, 1–20.

VINCENT, A. & MENEGUZZI, M. 1994 The dynamics of vorticity tubes in homogeneous turbulence. *J. Fluid Mech.* **258**, 245–254.

YAMAMOTO, K. & HOSOKAWA, I. 1988 A decaying isotropic turbulence pursued by the spectral method. *J. Phys. Soc. of Japan* **57**(5), 1532–1535.

ZEFF, B. W., LANTERMAN, D. D., MCALLISTER, R., ROY, R. & E. J. KOSTELICH, D. P. L. 2003 Measuring intense rotation and dissipation in turbulent flows. *Nature* **421**, 146–149.

ZHOU, J., ADRIAN, R. J., BALACHANDAR, S. & KENDALL, T. M. 1999 Mechanisms for generating coherent packets of hairpin vortices in channel flow. *J. Fluid Mech.* **387**, 353–396.